PS-11-04

Extended Abstracts of the 2019 International Conference on Solid State Devices and Materials, Nagoya, 2019, pp1005-1006

Sub 10nm Localized Thinning of Atomic Layers Tungsten Disulfide via In-situ STEM/TEM

Yi-Tang. Tseng[1], Kuo-Lun Tai[1] and Wen-Wei Wu[1]

[1] National Chiao Tung University
Department of Materials Science and Engineering
No.1001, University Rd., East Dist., Hsinchu City 30010, Taiwan
Phone: +886-3-5712121#55395 E-mail: wwwu@mail.nctu.edu.tw

Abstract

Two dimensional transitional metal dichalcogenides (TMDs) have been widely investigated in recent years for their electronic, optical and catalytic properties as well as specific mechanical properties. In fact, the characteristics mentioned above would be determined by the layer numbers or layer stacking configurations. Therefore, it is essential to design a method for developing new 2D-architecture by tailoring the properties of the material. In this work, we provided a sub 10nm localized thinning technique of atomic layers tungsten disulfide (WS_2) through in-situ scanning/transmission electron microscopy (STEM/TEM). The entire process was visualized at atomic scale and conducted at high temperature. With evidence provided by the TEM results, we successfully shaped the WS_2 layer by partially peeled off each WS_2 monolayer. Furthermore, we utilized atomic resolution STEM images to identify layer variation and structural configuration, which helped us deduce the exact atomic stacking sequence. This sculpting technique allows for sub-10nm thinning features while preserving the crystallinity, and also paves the way for the rational design of WS_2-based quantum and optoelectronic devices.

1. Introduction

Two dimensional transitional metal dichalcogenides (TMDs) have been widely investigated in recent years for their electronic[1], optical[2] and catalytic[3] properties as well as specific mechanical properties. In fact, the characteristics mentioned above would be determined by the layer numbers or layer stacking configurations. Therefore, it is essential to design a method for developing new 2D-architecture by tailoring the properties of the material. Recent research have shown great achievement in the atomic level observation of two-dimensional (2D) materials.[4, 5] However, real-time observation, which has been used to study layer evolution and edge reconstruction at atomic scale, remains a challenge.

In this research, we provided a sub 10nm localized thinning technique of atomic layers WS_2 via in-situ scanning/transmission electron microscopy (STEM/TEM). The entire process was visualized at atomic scale and conducted at 800◦C. To begin with, we shortly presented a methodical CVD system to synthesize the crystalline atomic-layers WS_2, followed by transferring the as-grown samples onto specialized TEM chips. Subsequently, with evidence provided by the TEM results, we successfully shaped the WS_2 layer by partially peeling off each WS_2 monolayer. Furthermore, we utilized atomic resolution STEM images to identify layer variation and structural configuration, which helped us deduce the exact atomic stacking sequence.

2. Experimental Section

The crystalline atomic-layers WS_2 were synthesized with a CVD method and grown on a SiO_2 (500 nm)/Si substrate. Afterward, the as-grown samples were transferred onto specialized TEM heating chips using a wet transfer process. The heating chip was then mounted on an in-situ TEM holder (Protochips Aduro300). The plane view of the sample is shown in Figure 1a, which is carried out in JOEL F200 TEM. The behavior of WS_2 localized thinning was performed at the temperature of 800℃.

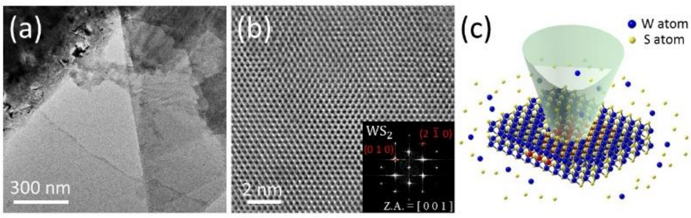

Fig. 1 (a) TEM image of the WS_2 sample before heating. (b) HRTEM image of (a) and inset shows corresponding FFT-DP with zone axis [001]. (c) schematic image of localized thinning.

2. Results and Discussion

Figure 1b demonstrates the high-resolution TEM image of the WS_2 sample, verifying the highly crystalline structure. Corresponding FFT-DP is also shown in inset. The sample was heated up to 800℃, and electron beam irradiation was conducted with an accelerating voltage of 200kV. As shown in Figure 2a,h, typical voids have been formed. Furthermore, void edges are terminated with zigzag lattice, which is considered to be stable and energetic preference.[6] A series of TEM images during the in-situ experiment was shown in figure 2b-g. The 5-layers tungsten disulfide has been etched by electron beam irradiation and peeled off layer by layer, which then becomes void rapidly. The dark contrast from 2D-behavior such as layer scrolling, folding and atoms aggregation can be observed in Figure 2h. In particular, the relatively thin area (indicated by red arrow) is found to be the result of partially layer peeled off during electron irradiation, in other words, localized thinning process.

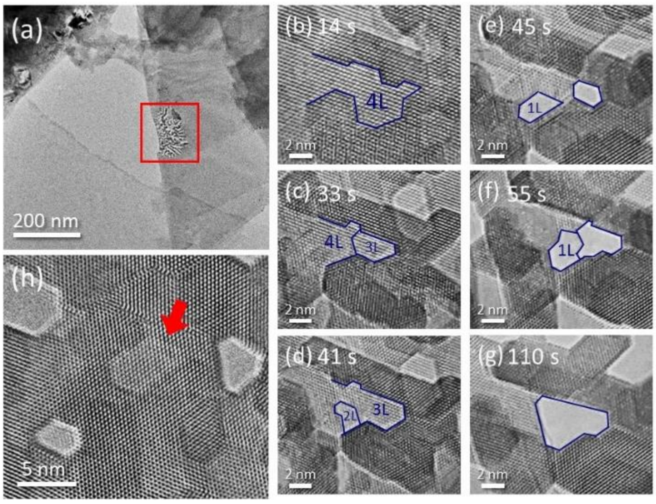

Fig. 2 in-situ TEM observation of layer thinning process from few-layers to voids and the localized thinning area found in HRTEM image. (a) TEM image of the WS_2 sample after heating (800℃). (b-g) Time sequencing HRTEM images of 5-layers WS_2 thinning via peeling off layer by layer.(h) HRTEM image from the selected area (red box in (a)), and the localized thinning area is pointed out by red arrow.

High resolution STEM image is used to deduce the exact atomic configuration during the localized thinning process. Figure 3 depicts some selected snapshots from the observed atomic-scale dynamics. The localized thinning process starts with the sulfur vacancy line (indicated by red arrow) shown in Figure 3a-c, which is caused by electron beam irradiation. Once the beam energy exceeds the knock-on damage threshold, the sulfur atom will be sputtered from the sheet.[7] As the sulfur vacancy line extended, we can observed the white contrast area formed. Since the energy for removing sulfur atom is lower than tungsten atom. When the sulfur atom is sputtered, the remaining tungsten atoms will aggregate and formed the cluster.

Figure 3d-g show the repair effect. When the beam energy exceeds the knock-on damage threshold, the atom will be sputtered from the sheet and form the vacancy line. However, the electron beam irradiation can also induce deposition.[8] If the repair rate is close to the sputtering rate, the expansion of etching area slows down. Moreover, the repair rate, which depends on the supply of the source material, is related to the number of layers. The sputter and repair process has repeated three times and lasts about 10 minutes.

3. Conclusions

We successfully synthesized the bilayer WS_2 with high crystallinity, and the WS_2 sample was heated up to 800∘C for real-time observation of electron beam irradiation. The void edge was found to be terminated by zigzag lattice. Localized thinning process took place and the exposed layer was observed because of different contrast in STEM image. In addition, we studied the connection of sputtering rate and repair rate via time series of STEM images and the variation of atomic configuration. This sculpting technique allows for sub-10nm thinning features while preserving the crystallinity, and also paves the way for the rational design of WS_2-based quantum and optoelectronic devices.

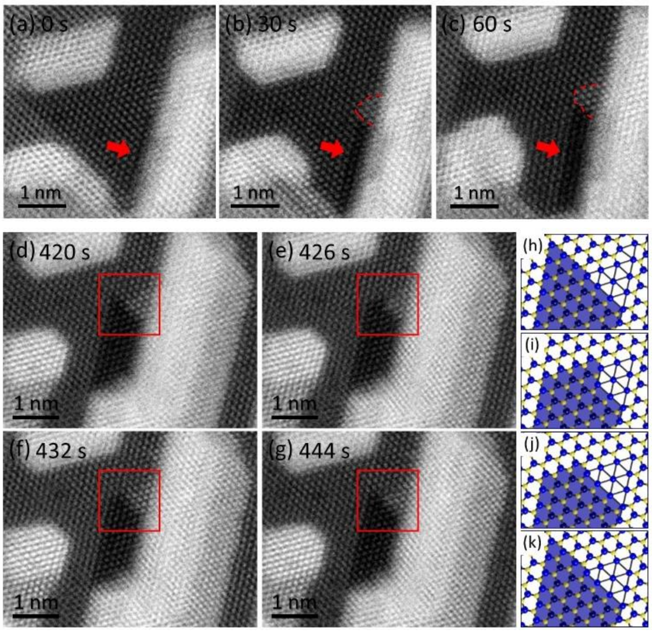

Figure 3. Atomic-resolved STEM images showing knock-on effect and repair mechanism during the few-layers (about 4 layers) WS_2 thinning process. (a-c) Time series of STEM images revealing the formation of vacancy line indicated by red arrow. The red dashed line distinguished the attached W cluster which has extended along with the vacancy line. (d-g) Time sequencing STEM images of thinning process follow by (a-c). Manually created atomic model of the red box in each frame is shown in (h-k). Tungsten and Sulfur atoms are represented by blue and yellow balls, respectively. The blue area is the exposed layer caused by etching.

References

[1] D. Ovchinnikov, A. Allain, Y.-S. Huang, D. Dumcenco, A. Kis, ACS Nano 8(8) (2014) 8174-8181.

[2] M.R. Molas, K. Nogajewski, A.O. Slobodeniuk, J. Binder, M. Bartos, M. Potemski, Nanoscale 9(35) (2017) 13128-13141.

[3] M.H. Siadati, M.P. De la Rosa, G. Berhault, J.P. Wilcoxon, R. Bearden, B.L. Abrams, Catalysis Reviews 48(1) (2006) 1-41.

[4] Y. Fan, A.W. Robertson, Y. Zhou, Q. Chen, X. Zhang, N.D. Browning, H. Zheng, M.H. Rümmeli, J.H. Warner, ACS Nano 11(9) (2017) 9435-9444.

[5] K.-L. Tai, G.-M. Huang, C.-W. Huang, T.-C. Tsai, S.-K. Lee, T.-Y. Lin, Y.-C. Lo, W.-W. Wu, Chemical Communications 54(71) (2018) 9941-9944.

[6] X. He, H. Li, Z. Zhu, Z. Dai, Y. Yang, P. Yang, Q. Zhang, P. Li, U. Schwingenschlogl, X. Zhang, 109(17) (2016) 173105.

[7] X. Liu, T. Xu, X. Wu, Z. Zhang, J. Yu, H. Qiu, J.-H. Hong, C.-H. Jin, J.-X. Li, X.-R. Wang, L.-T. Sun, W. Guo, Nature Communications 4 (2013) 1776.

[8] Y. Shen, T. Xu, X. Tan, L. He, K. Yin, N. Wan, L. Sun, 30(14) (2018) 1705954.